Available online at www.sciencedirect.com
SCIENCE DIRECT®
Proceedings of the Combustion Institute 30 (2005) 2667–2674
Proceedings of the Combustion Institute
www.elsevier.com/locate/proci

Quantitative in-cylinder NO-LIF imaging in a realistic gasoline engine with spray-guided direct injection

Wolfgang G. Bessler[a], Max Hofmann[a], Frank Zimmermann[a], Gerrit Suck[b], Jan Jakobs[b], Sascha Nicklitzsch[c], Tonghun Lee[d], Jürgen Wolfrum[a], Christof Schulz[e,*]

[a] *Physikalisch-Chemisches Institut (PCI), Universität Heidelberg, 69120 Heidelberg, Germany*
[b] *Volkswagen AG, 38436 Wolfsburg, Germany*
[c] *IAV GmbH, 09120 Chemnitz, Germany*
[d] *Department of Mechanical Engineering, Stanford University, Stanford, CA 94305, USA*
[e] *Institut für Verbrennung und Gasdynamik (IVG), Universität Duisburg-Essen, 47048 Duisburg, Germany*

Abstract

Limiting the in-cylinder nitric oxide (NO) formation is a crucial task in the development of engines with gasoline direct injection. Exhaust gas aftertreatment requires storage catalysts that tolerate a maximum NO flux only, and the frequency of energy consuming catalyst regeneration cycles is directly correlated with engine-out NO. We present quantitative in-cylinder imaging measurements of NO mole fractions in a gasoline engine with spray-guided direct injection using laser-induced fluorescence (LIF). The optical engine design was kept close to that of a serial four-cylinder engine. Optical access was achieved via sapphire windows, requiring only minor modifications to the engine block. The engine was operated with commercial gasoline and fired continuously. The data interpretation applies the spectral simulation tool *LIFSim* to calculate pressure, temperature, and gas-composition dependencies of the LIF signal. Temperature-dependent CO_2 absorption cross-sections are used to correct for laser and signal attenuation. A sensitivity analysis of the quantitative NO concentrations on the different parameters entering the evaluation is presented. The LIF measurements are compared to results from in-cylinder fast gas sampling through a modified spark plug. The two techniques show good quantitative agreement. The LIF measurements are also compared to charge-averaged working-cycle-resolved NO chemiluminescence measurements in the exhaust port. NO-LIF imaging results are presented for stratified engine operation with different levels of exhaust gas recirculation (EGR), showing the large impact of EGR on in-cylinder NO formation.

Keywords: Nitric oxide; Laser-induced fluorescence; Gasoline direct injection; Combustion diagnostics

1. Introduction

Gasoline engines with direct injection (DI) provide significantly increased energy efficiency compared to spark-ignition engines with multi-point injection in the intake port and are considered

* Corresponding author. Fax: +49 203 379 3087.
E-mail addresses: christof.schulz@pci.uni-heidelberg.de, christof.schulz@uni-duisburg.de (C. Schulz).

1540-7489/$ - see front matter © 2004 The Combustion Institute. Published by Elsevier Inc. All rights reserved.
doi:10.1016/j.proci.2004.08.123

the most favorable concept for spark-ignition engines in the near future. A problem of gasoline direct-injection engines is that conventional three-way catalysts do not work with excess oxygen that is present in the exhaust gases in stratified and homogeneous lean operation mode. Storage catalysts have been developed for exhaust gas aftertreatment of DI engines; they rely on successive storage and reductive operation modes. In the storage mode, nitric oxide (NO) is oxidized to NO_2 and chemically bound upon contact with the catalyst storage materials which must then be regenerated on a regular base by operating the engine under rich (reductive) conditions for a few working cycles. Because of restrictions in storage kinetics and capacity, the storage activity is limited in both maximum NO flux and accumulated amount of NO. Furthermore, the regeneration cycles are fuel consuming, and their frequency should be kept as low as possible. It is therefore crucial in engine development to minimize engine-out NO.

The requirement for the NO diagnostic approach presented here was to limit modifications in the engine and its operating conditions to the minimum possible. Sapphire was used as window material for optical access. Its stability allowed to reduce window thickness such that neighboring cylinders and water-cooling systems required no substantial modification. Commercial gasoline was used as fuel in the continuously running engine. This concept, however, also influences the diagnostic approach; e.g., sapphire windows prohibit the use of high laser energy densities at short wavelengths, and commercial fuel limits the UV transmission through unburned gases.

2. Background

Quantitative imaging of NO concentrations with laser-induced fluorescence (LIF) has attracted significant interest in recent years [1]. Measurements were performed in stable laminar flames [2] for developing and validating combustion models [3], and in gasoline and Diesel engines for in-cylinder diagnostics. The first applications were demonstrated in a spark-ignited square-piston engine fueled with propane [4]. More realistic configurations included engine operation with *iso*-octane with multi-point [5,6] and direct injection [7–9]. One-dimensional measurements were performed in an engine fueled with regular gasoline [5]. Quantitative NO-LIF imaging was also performed in Diesel engines fueled with low-sooting [10] and commercial Diesel fuel [11]. Quantitative interpretation of NO-LIF signals in realistic optical engines requires careful assessment of the influence of signal interference, pressure and temperature fluctuations, laser and signal attenuation, and calibration. These issues will be briefly discussed in this section. Additional details have been recently published [12–15].

2.1. Selective NO-LIF excitation and detection

Interference is an important issue in in-cylinder NO-LIF. O_2-LIF is the main contributor to interference in lean flames. CO_2-LIF was recently identified as a broad (200–450 nm) continuum in lean and rich flames [16]. Both the O_2-LIF/NO-LIF and CO_2-LIF/NO-LIF ratios increase with pressure because O_2 and CO_2 have a different pressure-dependence of fluorescence quantum yield and line broadening compared to NO [13]. In rich and non-premixed flames, additional broad-band fluorescence appears that is usually attributed to polycyclic aromatic hydrocarbons (PAH) [17]. The aromatic components of unburned commercial fuels strongly fluoresce, and interference with NO-LIF might be present especially in non-premixed engine operation.

Excitation wavelength and detection bandpass schemes that minimize interference for NO-LIF have been investigated in high-pressure flames [13–15]. The optimized strategy that is used here relies on A–X(0,2) excitation (O_{12} bandhead at 247.94 nm) with blue-shifted detection within the (0,0) and (0,1) band at 220–240 nm [8]. This scheme provides low O_2-LIF interference while minimizing the detection of PAH-LIF, CO_2-LIF, and fuel-LIF, all of which mainly fluoresce red-shifted compared to the excitation wavelength.

2.2. Dependence of NO-LIF signal on temperature, pressure, and gas composition

The dependence of NO-LIF on temperature T, pressure p, and species concentration x_i has been extensively studied. The main T-dependence arises from the population of the laser-coupled ground-state levels. T, p, and x_i also affect the frequency and cross-section of collisions that NO molecules encounter, influencing the excitation efficiency via broadening and shifting of the absorption lines [18,19], and the fluorescence quantum yield via collisional quenching [20,21]. These effects are calculated using the *LIFSim* software package [22].

Temporally resolved temperatures in internal combustion engines are usually not available. Quantitative NO measurements therefore require excitation of transitions that minimize the total T-sensitivity of the LIF signal. Figure 1 shows simulated NO-LIF signals versus T and p with 247.94 nm excitation and fixed NO *mole fractions*. The strong dependence of the signal on both parameters is evident; however, the calculations show that at high temperatures $\geqslant$2000 K the T-dependence is small [9,14]. Note this plot looks different for fixed NO *number densities*.

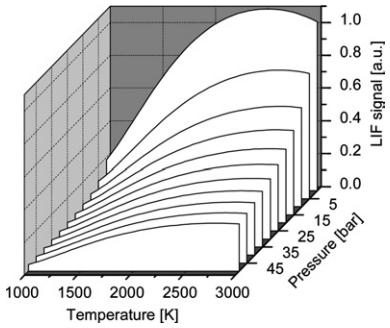

Fig. 1. Simulated NO-LIF signal strength versus temperature and pressure with excitation at the A–X(0,2) O_{12} bandhead at 247.94 nm, normalized to 1 bar, 2000 K.

The concentration of colliding species is even less available than T. The introduced error is, however, small for premixed combustion since NO is present only in the post-flame-front gases where the majority species concentrations are relatively precisely known. In diffusion flames, the required corrections can be as large as 25% [3]. The influence of local variations in air/fuel ratios observed in DI engines has been previously discussed [8].

2.3. Signal and laser attenuation

Electronic excitation of NO requires short UV wavelengths <250 nm [14]. Recent experiments show that in high-p, high-T combustion environments, UV light is attenuated by CO_2 [23]. Parametrized data are taken from [24]. The calculation of effective absorption cross-sections in inhomogeneous combustion situations is difficult since neither CO_2 nor T-distributions are known. Therefore, an accurate correction is often impossible in practical high-pressure flames, and attenuation remains a dominant source of uncertainty. We correct for attenuation of laser and LIF signal based on calculated CO_2 absorptivity (for details cf. Section 4.2).

2.4. Calibration

With the corrections considered above, NO-LIF is proportional to NO concentration, and absolute concentration requires calibration. While in situ calibration has been performed in engines under homogeneous lean conditions by adding NO to the feedstock gases [4,8,25] where ~90% of the NO survives the flame chemistry [26], technical restrictions due to the realistic engine setup prohibited this method in our experiments. Instead, we use a miniature calibration burner (20 cm long, 8-mm-diameter metal tube) that was inserted into the cylinder through the spark plug hole. A flat premixed methane/air flame was stabilized on the 7-mm-diameter matrix. The calibration information is obtained from LIF measurements with different amounts of NO up to 2000 ppm added to the premixed gases [9,12,25]. The temperature of this flame was characterized via multi-line NO-LIF thermometry [27].

3. Experimental

The experiments were carried out in a Volkswagen mass production four-cylinder FSI-engine that was originally designed for wall-guided direct-injection combustion (four valves, bore: 76.5 mm, stroke: 75.6 mm, engine displacement: 1390 cm^3). It was modified for spray-guided operation with a research high-pressure swirl-type injection system. The compression ratio was raised to 12.8:1, and the piston shape was modified. A 6-mm-high, 4-mm-thick sapphire ring that extends at one side into the side field of the pent-roof section provides optical access to the combustion chamber from three directions (Fig. 2). The total window area is comparatively small so that the wall-heat transfer is similar to the original engine.

The beam from a tunable KrF* excimer laser (*Lambda Physik*, $\Delta v = 0.6\ cm^{-1}$, 247.94 nm) was formed into a vertical light sheet of $4 \times 3\ mm^2$ with ~30 mJ prior to entering the engine. For each laser pulse, the energy was detected in front of and behind the engine by photodiodes (Fig. 3). LIF signals were imaged (*Halle*, $f = 100$ mm UV achromat) onto an ICCD camera (*LaVision* FlamestarIIF). NO-LIF was separated by reflection bandpass filters (eight dielectric 220–245 nm, 45° mirrors) and two 245 nm short-pass filters (*Laseroptik*). This filter combination yields a detection bandpass at 232 ± 8 nm (width at half maximum) with a transmission of ~35% at 225 nm (NO A–X(0,0) emission) and ~65% at 237 nm (A–X(0,1) emission) while suppressing elastically scattered light by six orders of magnitude.

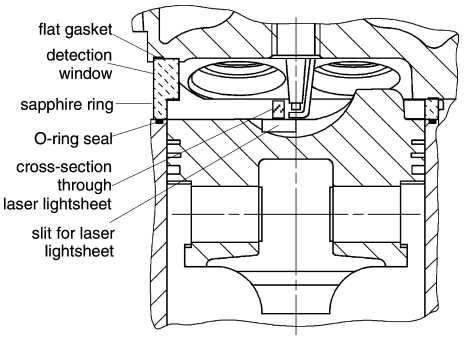

Fig. 2. Optically accessible four-cylinder engine with realistic piston and combustion chamber geometry.

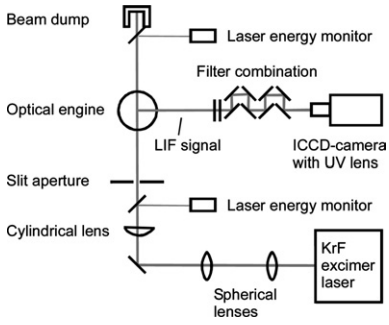

Fig. 3. Optical setup.

4. Results

4.1. NO-LIF selectivity

Excitation scans (247.85–248.00 nm) were measured in the fired engine in homogeneous operation at 20° and 60° crank angle after top dead center (CA ATDC) (Fig. 4). Calculated NO-LIF spectra can be fitted to the experimental data with *LIFSim* [22]. Free fit parameters are signal strength, baseline, and temperature. Background contributions (fitted baseline over simulated signal maximum) of 11% and 3% can be determined for 20 and 60°CA, respectively, showing the good interference suppression achieved with the present setup. In stratified operation mode, observed interference levels were slightly higher (~30% at 20°CA and <5% after 40°CA). Negligible signal (<1%) was measured when running the engine without ignition; thus, LIF from fuel components is almost completely suppressed with our detection strategy. The measurements shown in Fig. 4 were taken with a single laser pulse at each excitation wavelength position. The scatter in signal intensities therefore reflects the cycle-to-cycle fluctuations in NO-LIF signal. Nevertheless, fits to the spectra yield realistic temperatures (2400–2800 K) via multi-line NO-LIF thermometry [27].

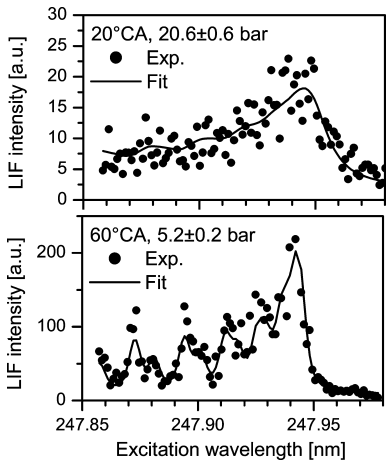

Fig. 4. LIF excitation scans in fired engine (homogeneous charge) and fits of simulated NO-LIF spectra to the experimental data.

4.2. NO-LIF quantification

An important parameter entering signal quantification is temperature. For the correction of the T-dependence of the NO-LIF signal and laser– and signal–light attenuation due to hot CO_2, we assume adiabatic flame temperatures (stoichiometric octane/air flame, $T \sim 2600$ K) for crank angles up to the 75% burned mass fraction (MFB, at ~15°CA ATDC with stratified operation). After 100°CA, mixing is assumed to provide a homogeneous T-distribution, and volume-averaged T calculated from pressure traces is used. Temperatures are linearly interpolated at intermediate CA. Accordingly, equilibrium CO_2 concentrations (for $\phi = 1.0$) are assumed for the burned gas zone until 75% MFB and interpolated down to measured exhaust CO_2 concentration (~5%) at 100°CA. The absorption path length has further influence on the total absorptivity. We assume a quasi-homogeneous, symmetric, linearly growing flame kernel, starting at 10% MFB (around −10°CA) that reaches a distance of 10 mm to the cylinder walls at 90% MFB (MFB points are evaluated individually for each operating condition from the in-cylinder pressure curves). Using these parameters, we perform corrections for laser– and signal–light attenuation based on T-dependent CO_2 absorption cross-sections [24]. The LIF images were corrected for laser and signal attenuation on a pixel-by-pixel basis (i.e., calculating correction factors for each point based on the respective laser and signal path lengths, and the respective wavelengths).

Figure 5 shows the relative variation of the NO-LIF signal of a given NO concentration as a function of crank angle for a spatial position in the center of the imaged volume. Dividing measured signal intensities by this factor yields

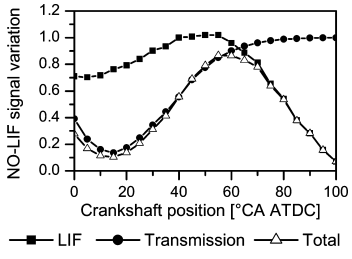

Fig. 5. Signal variation of a fixed NO concentration (stratified engine operation) versus crankshaft position and its contributions from LIF signal yield (normalized to 40°CA) and attenuation correction. The calibration (1900 K, 1 bar) condition corresponds to a LIF factor of 2.1 on this scale.

(non-calibrated) NO concentrations. Contributions from the LIF signal yield (Fig. 1) and attenuation are separated. From this figure, we can distinguish two regimes: Before 40°CA ATDC, the total correction is dominated by the laser and signal attenuation, while the LIF signal yield has a weak crank-angle dependence. After 60°CA, attenuation plays a minor role, but the LIF yield depends strongly on T.

The application of commercial fuel additionally limits the UV transmission through unburned gases. A correction is not attempted here. The measurements presented are therefore restricted to cases where the major part of the fuel is burned (later than ~20°CA ATDC), and light attenuation due to unburned fuel is neglected. Earlier experiments showed that signal attenuation due to NO (fluorescence trapping) is negligible [23].

4.3. Sensitivity and error analysis of NO-LIF quantification

Figure 6 shows a typical T-trace used in the data evaluation at stratified engine operation. A deviation from these values induces a variation in correction factors. For each crankshaft position, the T-range has been assessed that leads to a <10% and <25% variation of the correction factors. An extended T-range means low T-sensitivity. The LIF signal (Fig. 6A) is relatively T-insensitive for $T \geqslant 2000$ K. Knowledge of absolute temperatures as well as their local distribution in the burned gas is therefore not required at early combustion stages for correcting the LIF signal yield. However, laser and signal attenuation due to hot CO_2 is very T-sensitive, especially at high p and T (around 0°CA) (Fig. 6B). The total T-sensitivity is shown in Fig. 6C. We find that the effects of Fig. 6A and Fig. 6B partially compensate at 40–50°CA ATDC. We believe that real in-cylinder burned-gas temperatures are within the 25% NO variation limit (Fig. 6C) compared to the assumed temperatures.

Similar sensitivity analyses were performed for the assumed CO_2 concentration and the absorption path length. While the NO quantification is relatively insensitive to CO_2 concentration within limits that are reasonable for post-flame gases, the path length has a major influence on the attenuation correction at high p (0–30°CA ATDC). The lack of detailed information on flame growth in our simple approach makes this parameter a major source of uncertainty ($\geqslant$25%) before 30°CA.

The overall uncertainty in absolute NO mole fractions was estimated assuming the following parameter uncertainties: T: ±200 K, LIF yield: ±10% (mainly due to the uncertainty in gas composition affecting the quenching correction), x_{CO_2}: ±1%, flame radius: ±1 cm (both used in attenuation correction), and calibration: ±15%. Due to the non-linear coupling of the different parameters and their dependence on p, uncertainty varies strongly with crank angle (Fig. 7). At 40–70°CA ATDC, the uncertainties are around ±20%. Resulting error bars are shown in the figures.

4.4. Comparison of NO-LIF to in-cylinder gas sampling

A UV-analyzer [28] was used for NO concentration measurements in gas samples extracted from the combustion chamber at the spark plug location via a fast gas-sampling valve (GSV). GSV and NO-LIF measurements were applied under identical operation conditions with homogeneous charge ($\phi = 1.0$) used to reduce spatial and cycle-to-cycle fluctuations in NO concentrations. The valve has a sampling time of approx. 1 ms. Sampling is performed every sixth cycle, and the extracted gases mix before entering the detector. The measured data therefore represent a phase-averaged concentration over several working cycles.

Figure 8 shows a good agreement of in-cylinder NO concentrations obtained by LIF (phase-averaged over 60 instantaneous NO concentration fields) and the GSV technique. The remaining discrepancy before 30°CA ATDC may be explained with additional laser and signal attenuation due to unburned fuel, which is not corrected for, and by the difference in sample volumes (LIF: $18 \times 4 \times 3 = 216\ \text{mm}^3$ light sheet length × height ×

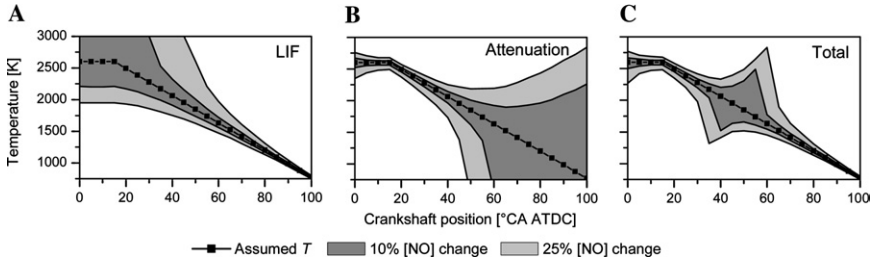

Fig. 6. Temperature sensitivity of NO-LIF quantification (stratified engine operation). Shown are the temperature values used in the data evaluation versus crank angle. The gray areas correspond to the temperature range that would result in a $\leqslant \pm 10(25)$% change in evaluated NO mole fraction. (A) LIF signal yield, (B) laser and signal attenuation, and (C) total T-sensitivity.

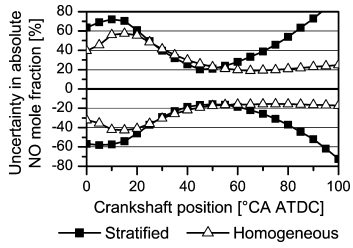

Fig. 7. Error analysis of NO-LIF quantification for stratified and homogeneous engine operation.

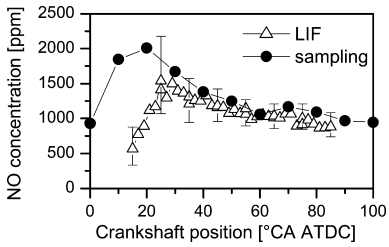

Fig. 8. Comparison of in-cylinder NO concentrations obtained with LIF and in-cylinder gas sampling. Homogeneous ($\phi = 1.0$) engine operation at 0.3 MPa indicated mean effective pressure (IMEP), 2000 rpm, 0% EGR.

width, GSV: ca. 500 mm^3, ca. 10 mm distance between the centers of both sample volumes).

4.5. Influence of exhaust gas recirculation on NO formation

NO-LIF imaging was used to investigate the influence of exhaust gas recirculation (EGR) on NO formation in stratified engine operation. EGR is an important technique to reduce engine-out NO. Its effect can be explained with an increased absolute heat capacity because of mixture dilution, lowering the in-cylinder burned-gas temperatures and thereby slowing the strongly T-dependent NO formation reactions [9]. Measurements with 0%, 20%, and 30% EGR (ratio of recirculated exhaust gas mass over total fed charge mass) at stratified engine operation (overall ϕ: 0.3–0.5 with increasing EGR) are shown in Figs. 9–11.

Instantaneous NO concentration fields for selected crankshaft positions at 20% EGR are shown in Fig. 9. The strong cycle-to-cycle fluctuation is evident. Surprisingly, fluctuations increase at later crankshaft positions. This is qualitatively visible in Fig. 9 and is confirmed when calculating the standard deviation of the single images, which increases from ~30% to ~80% between 20 and 80°CA ATDC for all studied EGR conditions. Given the relatively small LIF sampling volume compared to the cylinder dimensions, we interpret this observation as an effect of spatially inhomogeneous NO distributions (fluctuations in flame position and flow field) rather than cycle-to-cycle fluctuations in overall NO production.

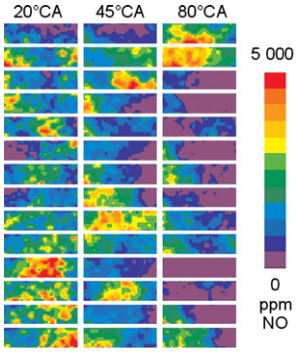

Fig. 9. Instantaneous NO concentration fields. Stratified ($\phi = 0.4$) engine operation, 20% EGR, 2000 rpm, 0.3 MPa IMEP. The images show an area of 14×4 mm^2.

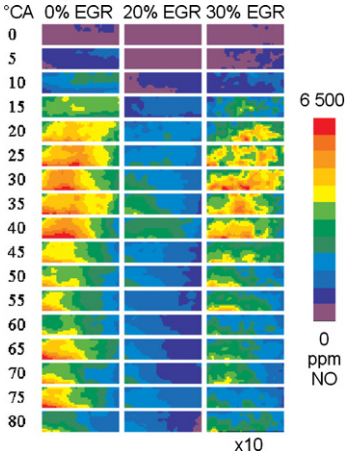

Fig. 10. Average NO concentration fields for different EGR ratio. Stratified ($\phi = 0.3$–0.5) engine operation, 2000 rpm, 0.3 MPa IMEP. The images show an area of 14×4 mm^2. At 30% EGR the look-up table is enhanced by a factor of 10.

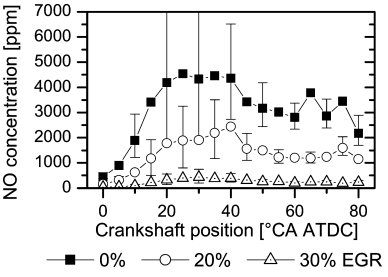

Fig. 11. Average NO concentrations from Fig. 10 for different EGR ratio.

Phase-averaged NO concentration fields (20 images per crankshaft position) are shown in Fig. 10. The strong reduction of NO concentration with increasing EGR ratio is evident. NO is

asymmetrically distributed even in these average images (note that the spark plug position is right behind the center of the imaged area, cf. Fig. 2). The laser travels from left (exhaust side) to right (intake side); nevertheless, the observed asymmetry is not an attenuation effect (which was corrected for in the data evaluation). Instead, it is more likely to find areas with high NO concentrations on the left side of the imaged area (location of exhaust valves). Spatially averaged NO concentrations from Fig. 10 are plotted versus crank angle in Fig. 11. Maximum NO concentrations in the imaged area occur around 30–40°CA ATDC. Note that concentrations are probably under-predicted at <20°CA due to laser attenuation by fuel vapor (cf. Section 4.2). At late crankshaft positions, the values are in qualitative agreement with the global NO emissions of 1200, 780, and 140 ppm NO for 0%, 20%, and 30% EGR, respectively, measured with the fast CLD analyzer. Additional operating conditions have been investigated, results are reported in [29,30].

4.6. Comparison of NO-LIF to exhaust port fast CLD measurements

To investigate further the cycle-to-cycle fluctuations in NO distribution, measurements were carried out in the exhaust port with a fast chemiluminescence detector (CLD) [31]. This allows a comparison between instantaneous NO-LIF concentrations obtained at arbitrary crankshaft positions and the charge-mass-averaged NO concentration [32] of the corresponding cycle.

Investigations were performed for stratified engine operation with different EGR ratio (Fig. 12). The correlation between the two techniques is evident when NO-LIF is measured at 20°CA ATDC. However, it is almost lost with NO-LIF at 80°CA. The observed scatter reflects the strong cycle-to-cycle fluctuations of NO concentration within the observed area at late crankshaft positions (cf. Fig. 9). Note that the uncertainty in LIF measurements is similar at these two crankshaft positions (Fig. 7). LIF probes only a small volume while the CLD results represent an average over the complete cylinder charge. A quantitative comparison of NO concentrations is therefore not possible. Instead, the LIF/CLD comparison confirms the image of strongly inhomogeneous NO distributions at late crank angles under stratified conditions. At the same time, the results show the importance of temporally resolved NO measurements at earlier detection times (around 20°CA ATDC), where observed fluctuations are directly correlated to engine out NO.

5. Conclusions

Laser-induced fluorescence of nitric oxide proved a viable technique for quantitative in-cylinder measurements of NO concentrations in a spray-guided DI engine with minimized optical accesses and operation with commercial gasoline. The major source of uncertainty arises from the unknown temperature and flame diameter that determine the correction for laser and signal attenuation. An overall accuracy of ±20–60% is estimated depending on crankshaft position. The comparison with in-cylinder sampling showed good agreement, and the comparison with exhaust port charge-averaged measurements confirms the image of a spatially very inhomogeneous in-cylinder NO distribution. The additional spatially and temporally resolved information of the NO imaging measurement is of high value for the understanding of the pollutant formation in DI gasoline engines. In this paper, we investigated the influence of exhaust-gas recirculation on NO formation under stratified engine operation. The peak NO concentrations decrease by a factor of 11 when increasing the EGR ratio from 0% to 30%.

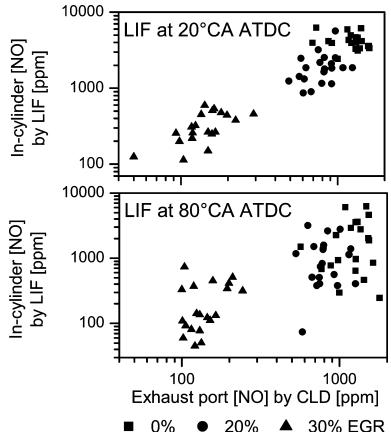

Fig. 12. Correlation of instantaneous NO-LIF concentrations (averaged over the imaged area) and exhaust port fast CLD measurements obtained from the corresponding working cycle. Note the double-log scale.

Acknowledgments

The technical support by U. Branczyk (PCI, Heidelberg), and T. Schindler and D. Lehmann (Volkswagen AG) is gratefully acknowledged. The Division of International Programs at the US NSF supports the traveling of T.L.

References

[1] J. Wolfrum, *Proc. Combust. Inst.* 27 (1998) 1–42.
[2] J.R. Reisel, N.M. Laurendeau, *Energy Fuels* 8 (1994) 1115–1122.
[3] J.B. Bell, M.S. Day, J.F. Grcar, W.G. Bessler, C. Schulz, P. Glarborg, A.D. Jensen, *Proc. Combust. Inst.* 29 (2002) 2195–2202.

[4] C. Schulz, V. Sick, J. Wolfrum, V. Drewes, M. Zahn, R. Maly, *Proc. Combust. Inst.* 26 (1996) 2597–2604.
[5] M. Knapp, A. Luczak, V. Beushausen, W. Hentschel, P. Manz, P. Andresen, *SAE Technical Paper Series* 970824 (1997).
[6] F. Hildenbrand, C. Schulz, V. Sick, G. Josefsson, I. Magnusson, Ö. Andersson, M. Aldén, *SAE Paper* 980148 (1998).
[7] P. Jamette, P. Desgroux, V. Ricordeau, B. Deschamps, *SAE Technical Paper Series* 2001-01-1926 (2001).
[8] F. Hildenbrand, C. Schulz, M. Hartmann, F. Puchner, G. Wawrschin, *SAE Paper* 1999-01-3545 (1999).
[9] W.G. Bessler, C. Schulz, M. Hartmann, M. Schenk, *SAE Technical Paper Series* 2001-01-1978 (2001).
[10] J.E. Dec, R.E. Canaan, *SAE Technical Paper Series* 980147 (1998).
[11] F. Hildenbrand, C. Schulz, J. Wolfrum, F. Keller, E. Wagner, *Proc. Combust. Inst.* 28 (2000) 1137–1144.
[12] W.G. Bessler, C. Schulz, T. Lee, D.I. Shin, M. Hofmann, J.B. Jeffries, J. Wolfrum, R.K. Hanson, *Appl. Phys. B* 75 (2002) 97–102.
[13] W.G. Bessler, C. Schulz, T. Lee, J.B. Jeffries, R.K. Hanson, *Appl. Opt.* 42 (2003) 2031–2042.
[14] W.G. Bessler, C. Schulz, T. Lee, J.B. Jeffries, R.K. Hanson, *Appl. Opt.* 42 (2003) 4922–4936.
[15] W.G. Bessler, C. Schulz, T. Lee, J.B. Jeffries, R.K. Hanson, *Appl. Opt.* 41 (2002) 3547–3557.
[16] W.G. Bessler, C. Schulz, T. Lee, J.B. Jeffries, R.K. Hanson, *Chem. Phys. Lett.* 375 (2003) 344–349.
[17] A. Cialolo, R. Barbella, A. Tregrossi, L. Bonfanti, *Proc. Combust. Inst.* 27 (1998) 1481–1487.
[18] A.Y. Chang, M.D. DiRosa, R.K. Hanson, *J. Quant. Spectrosc. Radiat. Transfer* 47 (1992) 375–390.
[19] M.D. DiRosa, R.K. Hanson, *J. Quant. Spectrosc. Radiat. Transfer* 52 (1994) 515–529.
[20] P.H. Paul, J.A. Gray, J.L. Durant Jr., J.W. Thoman Jr., *Appl. Phys. B* 57 (1993) 249–259.
[21] P.H. Paul, J.A. Gray, J.L. Durant Jr., J.W. Thoman Jr., *AIAA J.* 32 (1994) 1670–1675.
[22] W.G. Bessler, C. Schulz, V. Sick, J.W. Daily, in: *Proceedings of the 3rd Joint Meeting of the US Sections of the Combustion Institute*, Chicago, 2003, PI1-6. Available from www.lifsim.com.
[23] F. Hildenbrand, C. Schulz, *Appl. Phys. B* 73 (2001) 165–172.
[24] C. Schulz, J.B. Jeffries, D.F. Davidson, J.D. Koch, J. Wolfrum, R.K. Hanson, *Proc. Combust. Inst.* 29 (2002) 2725–2742.
[25] C. Schulz, V. Sick, U.E. Meier, J. Heinze, W. Stricker, *Appl. Opt.* 38 (1999) 434–1443.
[26] P.A. Berg, G.P. Smith, J.B. Jeffries, D.R. Crosley, *Proc. Combust. Inst.* 27 (1998) 1377–1384.
[27] W.G. Bessler, C. Schulz, *Appl. Phys. B* 78 (2004) 519–533.
[28] B. Heller, G. Lach, J.D. Baronick, W. Fabinski, M. Moede, *SAE Technical Paper Series 2004-01-1830* (2004).
[29] G. Suck, J. Jakobs, S. Nicklitzsch, T. Lee, W.G. Bessler, M. Hofmann, F. Zimmermann, C. Schulz, *SAE Paper* 2004-01-1918 (2004).
[30] G. Suck, J. Jakobs, S. Nicklitzsch, W.G. Bessler, Max Hofmann, C. Schulz, in: *International Symposium on Internal Combustion Diagnostics*, Baden-Baden, 2004.
[31] R. Ford, N. Collings, *SAE Paper* 1999-01-0208 (1999).
[32] J.K. Ball, C.R. Stone, N. Collings, *Proc. Inst. Mech. Eng.* 213 (D) (1999) 175–189.

Comments

Volker, Sick, University of Michigan, USA. Are cyclic variations in NO formation a significant source for overall NO levels emitted by the engine?

Reply. Figure 12 shows cycle-resolved measurements of the charge-mass-averaged NO concentration measured in the exhaust port of the engine by a fast chemiluminescence detector. From the upper diagram we derive the following relative standard deviations of 21, 24, and 33% at 0, 20, and 30% EGR rate, respectively. There is indeed a strong cyclic variation of the overall NO emission which increases with increasing EGR-rate.

•

Michael Drake, General Motors, USA. You are measuring NO LIF in a narrow region (4×14 mm) in this highly stratified engine, but you still get good correlations with in-cylinder sampling from a different region in the cylinder and from exhaust gas measurements. How widely applicable do you think this is?

Reply. The comparative measurements between NO-LIF and gas-sampling-valve (GSV) technique (Fig. 8) were carried out under homogeneous operating conditions with early fuel injection in order to minimize local variations in mixture properties and combustion progress. The GSV system can neither perform instantaneous measurements (valve opening time ca. 1 ms) nor cycle-resolved measurements (about 100 cycles are sampled). Therefore, the NO-LIF concentration results were similarly averaged (data averaged over one millisecond and the data of 20 engine-cycles) in order to compare both techniques. The NO-LIF technique, however, additionally provides spatially and temporally resolved measurements. The local variations under stratified conditions are shown in Fig. 9. Under these conditions a sampling measurement would not yield useful data for a comparison.

The correlation between in-cylinder NO-LIF and exhaust gas measurement is relatively poor on a cycle resolved basis. At 20 °CA ATDC (Fig. 12) we observe a good correlation on a statistical basis. This is plausible because with stratified-charge operation and the combustion (and hence, NO formation) mainly takes place in the vicinity of the spark plug where the NO-LIF sampling volume was located. Under these conditions, the volume observed by NO-LIF represents the total load relatively well.